Rapid, selective and single cell electrical detection of antibiotic resistant bacteria

Narendra Kumar[1†], Wenjian Wang[3†], Juan C. Ortiz-Marquez [2†], Matthew Catalano[1], Mason Gray[1], Nadia Biglari[1], Kitadai Hikari[4], Xi Ling[4], Jianmin Gao[3]*, Tim van Opijnen[2]*, Kenneth S Burch[1]*

[1]Department of Physics, [2]Department of Biology, [3]Department of Chemistry, Boston College, Chestnut Hill, Massachusetts 02467, United States

[4]Department of Chemistry, Boston University, Boston, Massachusetts 02215, United States

Corresponding Authors

*Email: ks.burch@bc.edu

*Email:vanopijn@bc.edu

*Email:gaojc@bc.edu

† These authors contributed equally.

ABSTRACT

Time-consuming, expensive and low sensitivity diagnostic methods used for monitoring bacterial infections lead to unnecessary or delays in prescription of the right antibiotic treatment. Determining an optimal clinical treatment requires rapid detection and identification of pathogenic bacteria and their sensitivity to specific antimicrobials. However, diagnostic devices that meet all of these criteria have proven elusive thus far. Graphene field effect transistors (G-FET) are a promising solution, since they are highly sensitive to chemical/biological modification, can have fast detection times and can be placed on different substrates. Here, by integrating specific peptide probes over G-FETs, we present a proof-of-concept study for species and strain specific label-free detection of clinical strains of pathogenic bacteria with high specificity and sensitivity. We found that pyrene-conjugated peptides immobilized on G-FETs were capable of detecting pathogenic *Staphylococcus aureus* at the single-cell level and discriminate against other gram-positive and gram-negative bacterial pathogens. A similar device was able to discriminate between antibiotic resistant and sensitive strains of *Acinetobacter baumannii*, suggesting that these devices can also be used for detecting antibiotic resistive pathogens. Furthermore, a new means of enhancing attachment, electric-field assisted binding, reduced the detection limit to 10^4 cells/ml and the detection time to below 5 minutes. The combination of single step attachment, inexpensive production, rapid, selective and sensitive detection suggest G-FETs plus pyrene-conjugated peptides are a new platform for solving major challenges faced in point of care diagnostics to fight infectious diseases and antimicrobial resistance.

KEYWORDS: Biosensors, G-FET, Peptide probes, Antibiotic Resistance Bacteria, Electrical detection, Dirac Voltage

Bacterial infections cause a wide range of diseases and significant mortality[1]. While antibiotics are key in controlling disease severity and reducing mortality, their over prescription and misuse are some of the most important factors in the surge of antibiotic resistant cases around the world.[2-4] In order to solve this crisis, diagnostic methods are needed that can rapidly and accurately identify the bacterium causing the infection and determine its associated antibiotic resistance profile. Antibiotic susceptibility testing (AST) is mostly carried out by phenotypic methods that require prior identification of bacterial pathogens from patients (at the species and/or strain level) and incubation under antibiotic conditions,[5, 6] a lengthy process that can take up to 24 hours to a month depending on the species.[7] Moreover, both species/strain identification and AST require trained specialists, specific laboratory environments and often expensive instrumentation.[5, 6, 8] Since these conditions limit widespread application and implementation into actual treatment strategies at most points of care, there is much room for improvement to develop new diagnostic devices that have the potential for adoption across a large variety of use cases. Ideally these devices would be cheap, easy to implement, scalable, and accurately identify both the pathogen as well as its antibiotic resistance profile with high specificity and sensitivity.[9-11]

Graphene field effect transistors (G-FETs) have been gaining attention due to their high sensitivity in detection of biomarkers and DNA, scalability, biocompatibility and ease of incorporation on conventional and flexible substrates.[12-15] However, the use of G-FET sensors for bacterial detection is still in its infancy with only a small number of papers describing the detection of a lab strain of *Escherichia coli*, but no reports on the sensing of clinically relevant pathogenic bacteria, nor on antibiotic resistant strains.[16-18] An impediment to the broad use of G-FETs for bacterial sensing lies in the lack of suitable probes which should be readily available, easily handled (simple preparation and/or long shelf life), and strain-specific.[19, 20] An equally crucial

challenge is enhancing the sensitivity to achieve detection at a clinically relevant cell density. This is limited, in part, by the typical large charge and size of most probes. As such the probes strongly shift the Dirac voltage (point of charge neutrality - V_D), or keep the target beyond the Debye screening length, such that only small changes in electrical resistance are observed upon attachment.[21] Indeed, most studies have relied on changes in source-drain current, due to relatively small shifts in V_D upon attachment. This results from the fixed amount of charge per cell, whereas the shift is dependent on the induced charge density.[18] As such the effect of the bacteria on a single G-FET could be enhanced with smaller active areas, however this also requires a far higher cell density, potentially at a level that is much above what is considered to be clinically relevant. Nonetheless, enabling further reduction of the needed active area, would also allow for multiplexing by placing in the sample space numerous G-FET elements with a variety of probes.

Herein, we report a new design of G-FET sensors and protocol for their implementation with diverse pathogenic bacterial species. Specifically, we utilize specially selected synthetic peptides as probes for bacterial capture and push the bacteria to the graphene with electrical pulses to lower the limit of detection to 10^4 cells/ml (within a clinical relevant regime) and the time of detection to 5 minutes. We produced peptides conjugated with pyrene, enabling simple one step non-covalent functionalization on G-FETs that can be stored at room temperature for weeks. The chemically modified peptides used in this work are relatively inexpensive to produce and solve the issue of lower level of selectivity for instance observed with antimicrobial peptides.[22-26] The peptides also provide an advantage over antibodies or aptamers, namely their small size and neutral (no net charge) state.[22, 24, 27, 28] This results in large changes in V_D per bacteria, allowing for single cell electrical detection on G-FET. Importantly, our G-FET design enabled direct quantitative comparison of the electrical and optical readout by simple optical imaging of G-FET. Combined

with a new method of applying gate pulses to push the bacteria to the graphene, we overcame the tradeoff between the probability of attachment and V_D shift per bacteria. The wide applicability of these peptide probes enabled detection of different pathogenic bacterial species, as well as an antibiotic resistant strain at a single cell level. Thereby our G-FET plus peptide combination offers a new promising route towards cheap, fast, multiplexed and low concentration detection of clinically relevant pathogenic bacterial species and their antibiotic resistant variants.

RESULTS AND DISCUSSION

G-FET device construction and baseline measurements.

G-FET devices consist of a low pressure chemical vapor deposition (CVD) graphene on a standard SiO_2/Si substrate, and etched into an active area of 20 x 50 µm, with Cr/Au source and drain. The contacts were passivated and the sensing area (10 x 40 µm) was defined easily with a conventional hard baked photoresist (S1805), instead of a dielectric (Figure 1a). To measure the baseline conductance/resistance of a device, they were tested in liquid gate mode where a Pt wire was chosen as reference electrode and 0.01x PBS as electrolyte (Figure 1b). The measured average Dirac voltage (V_D) of the fabricated G-FETs is around 0.7±0.16 V, consistent with the surface potential of the platinum wire and diluted concentration of phosphate buffer saline (PBS).[29] The observed variation in the V_D with devices made on various substrates and batches is attributed to the impurities at the graphene/SiO_2 interface induced during the graphene transfer process. The mobility was calculated by linearly fitting the hole and electron regimes of conductance (σ) versus voltage (V_G) using $\mu = \frac{L}{W}\frac{1}{C_{LG}}\left(\frac{\partial\sigma}{\partial V_G}\right)$, where L, W are the length and width of the channel, C_{LG} is the liquid gate capacitance. Value of C_{LG} was taken to be 1.65 µF/cm^2 based on the sum of the quantum capacitance (C_Q) of graphene and electric double layer capacitance (C_{DL}) consistent with 0.01x PBS.[18] Results from a high mobility device are shown in Figure 1b, while the average hole

and electron mobility values obtained from different devices are ~670 ± 125 and ~690 ± 83 $cm^2/V \cdot s$, respectively. These mobilities are consistent with reported values for CVD graphene on SiO_2 substrates.[18, 30]

Bacterial detection using G-FETs with bare graphene.

To ensure the dimensions of the device and operating conditions would detect bacteria, we first exposed a bare G-FET containing a strip of non-functionalized bare graphene to two types of bacteria: *E. coli* and *Staphylococcus aureus*. Each species was incubated for 45 minutes on different devices at a bacterial suspension of 10^7 cells/ml. As evident from Figure 1c, a strong shift in V_D of 360 mV results from exposure to *E. coli* and 220 mV from *S. aureus* (Figure S1). This positive shift by attachment of *E. coli* is consistent with that observed in back gate mode.[31] These results confirm that our bare graphene is highly sensitive to the bacterial surface charge but cannot distinguish between different bacterial species, strains or resistance state, indicating that G-FET's require specific probes to be integrated on such devices.

Peptide-pyrene conjugates enable a simplified single-step graphene functionalization process.

In order to maintain the electronic properties of graphene, it is preferable to use probes with non-covalent functionalization through π-π stacking of pyrene-based linker molecules.[32] This functionalization typically requires multiple steps, starting at linker attachment and followed by incubation with biosensing probes. As a result, G-FETs are exposed to different solvents with the potential of significantly affecting the doping level of the graphene.[13, 14, 33] This also makes the preparation and functionalization of devices complex, cumbersome, and potentially expensive. Previously we developed a phage display platform that can rapidly select for small peptides that recognize and bind specific bacterial species or strains.[34] KAM5 is one such peptide that was identified in our previous study to specifically detect *S. aureus*, showing an EC_{50} of ~1.5 μM in a

cell staining assay. To minimize exposure of G-FET to solvents and facilitate single step functionalization with the desired probe, we synthesized a peptide-pyrene conjugate (P-KAM5_Probe), by on-resin coupling of 1-pyrenebutyric acid N-hydroxysuccinimide ester (PBASE) onto the diaminopropionic acid residue installed at the C-terminus of the peptide. These pyrene-conjugated peptides are then simply dissolved in aqueous solution incubated on the device for 2 hours followed by a wash step, with no additional chemicals or treatments required. In order to confirm uniform functionalization, P-KAM5_Probe was attached to the patterned bare graphene surface and characterized with atomic force microscopy (AFM; Figure 1d). The height of graphene functionalized with P-KAM5_Probe increased by ~2.5 nm as compared to the bare graphene surface. This height increase is expected and consistent with peptides attached to carbon nanotubes or graphene oxide,[35, 36] confirming the attachment of the probe to the device. The peptide-pyrene conjugates thus facilitate simplified graphene functionalization by a single step process, which enables rapid and easy preparation of the device as well as reduced fabrication cost. Raman spectrum was carried out to confirm the quality of the CVD graphene used for the G-FET fabrication (Figure 1e). Obtained 2D peak at 2,679 cm^{-1} and G peak at 1,587 cm^{-1} with the ratio in their intensities i.e. I_{2D}/I_G ~1.6, confirming the single layer graphene, while the absence of D peak ~1350 cm^{-1} indicating defect free graphene.[37]

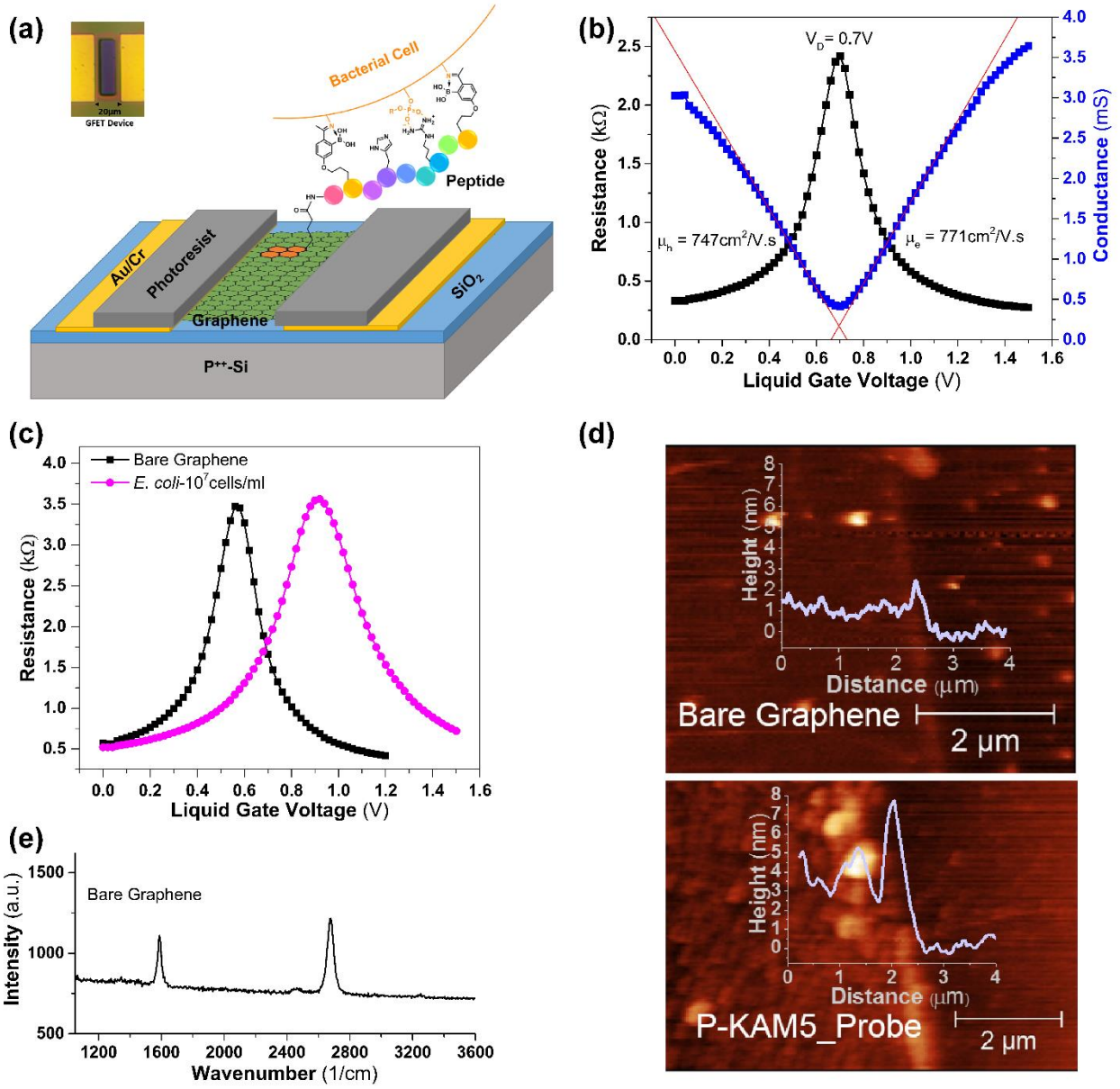

Figure 1. Scheme of functionalization and characterization of G-FETs *(a) A schematic of a G-FET functionalized with a pyrene-conjugated peptide probe binding to the surface of a bacterium. The inset shows a light microscopy image of G-FET, with an active area of 10 x 40 μm, located in between two gold contacts. (b) Resistance/conductance vs voltage plots of G-FET representing the Dirac voltage (0.7 V), hole and electron mobilities of 747 and 771 cm^2/V.s. (c) G-FET characteristics before and after adsorption of E. coli. A shift of 360 mV in the Dirac voltage observed when G-FET with bare graphene was incubated with E. coli (pink circles) in comparison with the bare graphene (black squares). (d) AFM image of the patterned graphene before and after peptide functionalization. After functionalization, the coverage of the graphene channel by the P-KAM5-peptide probe is shown as an increase in height of ~2.5 nm (lower panel) compared with the bare graphene surface (upper panel). (e) Raman spectrum (532 nm excitation) of CVD graphene transferred over SiO_2/Si substrate. The spectrum shows 2D peak at 2,679 cm^{-1} and G*

peak at 1,587 cm^{-1} with I_{2D}/I_G ~1.6, suggesting the graphene is monolayer. Absence of D peak ~1350 cm^{-1} indicating defect free graphene.

Species specific detection of a Gram-positive bacterial pathogen.

To test the potential of our G-FET design for detecting specific bacterial species, we functionalized G-FETs with P-KAM5_Probe, which is expected to bind *S. aureus*, or a control peptide (P-KAM5_Control, see Supporting Information for details), in which the key functional groups for binding are missing thereby making it incapable of binding bacteria. As shown in Figure 2a-b, functionalization of G-FET with either peptide does not show any shift in V_D, consistent with their charge neutral structure at pH 7. Upon incubation with *S. aureus* at 10^7 cells/ml on a GFET functionalized with P-KAM5_Probe a voltage shift of 300 mV was observed (Figure 2a). In contrast and as expected, no notable voltage shift was observed when *S. aureus* was incubated on devices functionalized with P-KAM5_Control (Figure 2b). To visually confirm that the shift in V_D is due to bacteria attached to the surface of the graphene, devices were analyzed using optical microscopy. *S. aureus* is a spherically shaped bacterium with an approximate 1 μm diameter,[38] and black dots, representing individual bacterial cells, were observed only on devices functionalized with P-KAM5_Probe and not P-KAM5_Control (inset of Figure 2a-b). The observed positive shift in the V_D is attributed to the negatively charged surface of bacterial cells which increase the hole carrier density in graphene.[18] To probe the postulated *S. aureus* specificity of our G-FET, the peptide functionalized devices were comparatively tested against *Bacillus subtilis* a different Gram-positive species and *E. coli* a representative Gram-negative bacterium. No significant shift in V_D was observed when the devices were incubated with either species under the same conditions used for *S. aureus* (Figure 2c). Importantly, after rinsing with DI, the same devices were subsequently incubated with *S. aureus* resulting in an average shift in V_D of ~190 mV, indicating

that the devices functionalized with P-KAM5-probe are specific to *S. aureus* and insensitive to other Gram-positive and negative species.

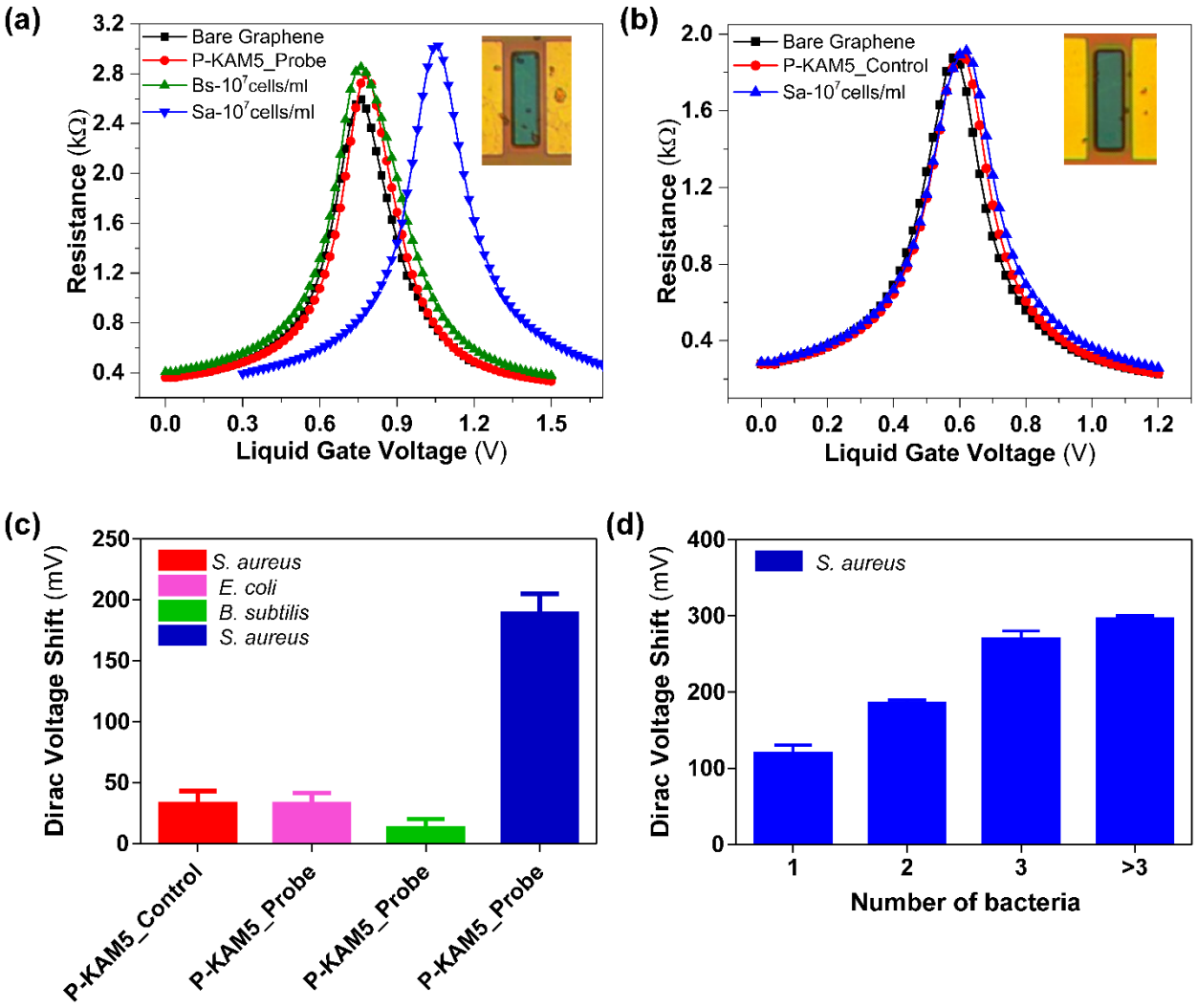

Figure 2. Specific detection results of S. aureus. *Resistance vs voltage plots of G-FET for detection of S. aureus (a) G-FET functionalized with Probe peptides (P-KAM5_Probe) and incubated with B. subtilis and S. aureus at a concentration of 10^7cells/ml. No shift was observed with peptides and B. subtilis while a shift of ~300 mV is seen with S. aureus as well as the attachment of bacterial cells to the graphene (see image in inset). (b) G-FET functionalized with control peptides (P-KAM5_Control) and incubated with S. aureus at a concentration of 10^7 cells/ml. No voltage shift was observed after the incubations with peptide as well as with bacteria. Additionally, no attachment of bacterial cells on the graphene was observed (see image in inset). (c) Comparative values of average voltage shift with specific and unspecific detection of S. aureus. No notable shift was observed when G-FET were functionalized with P-KAM5_Control and incubated with S. aureus at a concentration of 10^7 cells/ml. Furthermore, no notable shift was observed when G-FET were functionalized with P-KAM5_Probe and incubated with unspecific*

bacteria (E.coli and B. subtilis) at a concentration of 10^7 cells/ml. An average shift of ~190 mV was observed when G-FET functionalized with P-KAM5_Probe and incubated with S. aureus at a concentration of 10^7 cells/ml. (Data represents average and standard deviation of at least 6 independent replicates) (d) Measured Dirac voltage shift of G-FETs having different number of bacteria (S. aureus) attached. Devices having single bacterium attached show an average shift of ~130 mV and linear increase in voltage shift is observed with increased number of bacteria attached. (Data represents average and standard error of at least 3 independent replicates).

Additional correlation was found by using optical imaging to count the number of bacteria on each G-FET after electrical detection. Specifically, after measuring 20 devices functionalized with P-KAM5_Probe and incubated with *S. aureus* followed by inspection with light microscopy it was observed that a strong correlation exists between the number of bacteria that are bound by the probe to the graphene and the registered voltage shift. As shown in Figure 2d, a linear shift of V_D was seen with increasing number of attached bacteria with a sensitivity of 56.3 ± 7.3 mV/bacteria. Surprisingly, the devices are able to detect the attachment of a single bacterium with an average voltage shift of 128±18 mV, a nearly 20% increase in the measured V_D over the as-prepared G-FET. Moreover, the voltage shifts of ~130 → 300 mV (Figure2d) that were obtained are much higher than those reported for *S. aureus* (~25 mV) and *E. coli* (~60 mV) using silicon based FET sensors.[39, 40] There are two crucial reasons for this prominent readout. First, the peptide-probes that are implemented here are small in size (~2.5 nm) and have a neutral charge that reduces the Debye screening effect and background signal, respectively. Second, the small device size (10 x 40 µm) and the measurements at the charge neutrality point enhance the sensitivity of the graphene to the charge of the bacteria. Altogether, these results confirm that G-FETs functionalized with P-KAM5_Probe are capable of detecting *S. aureus* with high specificity and sensitivity, at the single cell level. Additionally, the peptides functionalized over G-FET remains stable tested after storing for 24 hours in PBS which showed detection capability similar to those used immediately after functionalization (Figure S2).

Improving sensitivity via electric-field assisted bacterial binding.

One potential problem associated with our design is the relatively small size of the device, which requires a high bacterial cell density (10^7 cells/ml of *S. aureus*) to facilitate the capture of a single bacterium at the graphene surface. The active area of our G-FET is just 10 x 40 µm, while bacterial cells are distributed in an area of 2.5 x 2.5 mm, which is the size of the PDMS well placed over the device and which holds the bacterial suspension. We hypothesized that this dramatic contrast between the size of the well and that of the graphene limits the likelihood of the bacterial cells reaching the graphene surface, therefore requiring a high cell density for efficient bacterial capture. To improve the sensitivity of G-FET, we hypothesized that by applying voltage pulses from the top of the well that holds the sample, the charge of the bacteria could be exploited to drive them to the graphene surface.[41] Specifically, a negative voltage of -0.5 V was applied to the Pt electrode with five pulses, 10 seconds in duration to minimize potential damage to the bacteria. Figure 3 shows a clear shift in V_D after electric field assisted binding at a concentration of 10^5 and 10^4 cells/ml of *S. aureus* respectively, indicating attachment of bacteria to the graphene. Moreover, electric-field assisted binding decreased the original incubation time before bacteria could be detected from 45 minutes to 5 minutes. Similar to the 45 min incubation method without electric field attachment, the Dirac voltage shift found in the electric-field assisted attachment is dependent on the number of bacteria on the device (Figure S3). Excitingly, our newly developed method of electric field assisted binding allows effective detection of *S. aureus* at 10^4 cells/ml, which is 3 orders of magnitude lower in cell density than what is required in the absence of applying voltage pulses. Moreover, it also reduces the time needed to perform the measurements by 9-fold. To make sure that the selectivity of the devices is not affected by applying the voltage, we tested *B. subtilis*

and *E. coli* using P-KAM5_probe devices, and *S. aureus* using P-KAM5_Control. No shift or bacterial attachment was observed after applying the voltage (Figure S4).

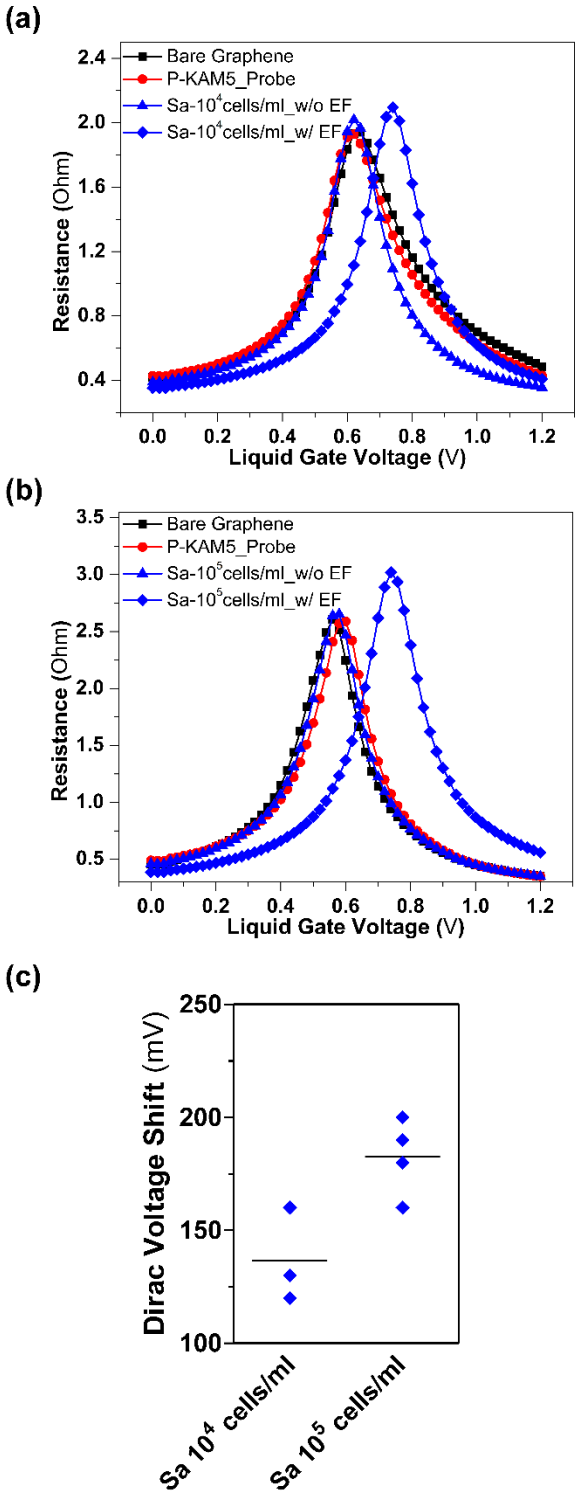

Figure 3. Lowering detection with electric field assisted binding. *Resistance versus voltage plots of G-FET functionalized with Probe peptides (P-KAM5_Probe) before (blue triangle) and after (blue diamond) electric field (EF) assisted binding of S. aureus at 10^4 cells/ml (a) and 10^5 cells/ml (b). (c) The chart shows the Dirac voltage shift and average obtained with two concentrations of S. aureus after electric field assisted binding.*

Strain specific detection of Gram-negative antibiotic resistant pathogenic bacteria.

The use of peptide probes in our G-FET design offers great versatility in terms of bacterial pathogens that can be targeted. Furthermore, as we recently demonstrated, the peptide probes can be rapidly developed to differentiate antibiotic susceptible and antibiotic-resistant strains of a bacterial pathogen. We postulated that integrating such peptide probes into G-FET would allow for specific detection of antibiotic-resistant pathogenic strains. To test this hypothesis, we turned to the peptide KAM8, which was selected to bind a colistin-resistant strain of *Acinetobacter baumannii* (AB5075 LOS−;AbR). Similar to the P-KAM5_Probe, we synthesized a pyrene conjugate of KAM8 P-KAM8_Probe as well as a control peptide (P-KAM8_Control). Functionalizing G-FET with P-KAM8_Probe or P-KAM8_Control caused no shift in V_D (Figure 4a) confirming their charge neutrality. After incubation with 10^7 cells/ml of AbR, a V_D shift ranging between 280-460mV was observed for devices functionalized with P-KAM8_Probe (Figure 4a) while no notable shift was measured with P-KAM8_Control (Figure S5). This shows that P-KAM8_Probe effectively captures AbR cells onto the graphene surface triggering a change in V_D. In order to confirm the strain specificity of P-KAM8_Probe, the devices were first incubated with the non-colistin resistant wild-type strain of *A. baumannii* (AB5075; AbW) at 10^7 cells/ml. This triggered no shift in Dirac voltage indicating that P-KAM8_Probe does not interact with the strain. Subsequently, the same device was incubated with the antibiotic-resistant strain AbR which showed a shift of 280mV confirming the probe interacting with AbR. Additionally, similar to what was observed for the interaction between *S. aureus* and P-KAM5_Probe, the measured voltage

shifts correlate with the number of bacterial cells attached to the graphene surface (Figure S6). We found a single *A. baumannii* produced a V_D shift of ~200mV, which is comparatively higher than that obtained with *S. aureus* which likely results from a higher density of surface charge displayed by a Gram-negative bacterium in comparison to Gram-positives.[42]

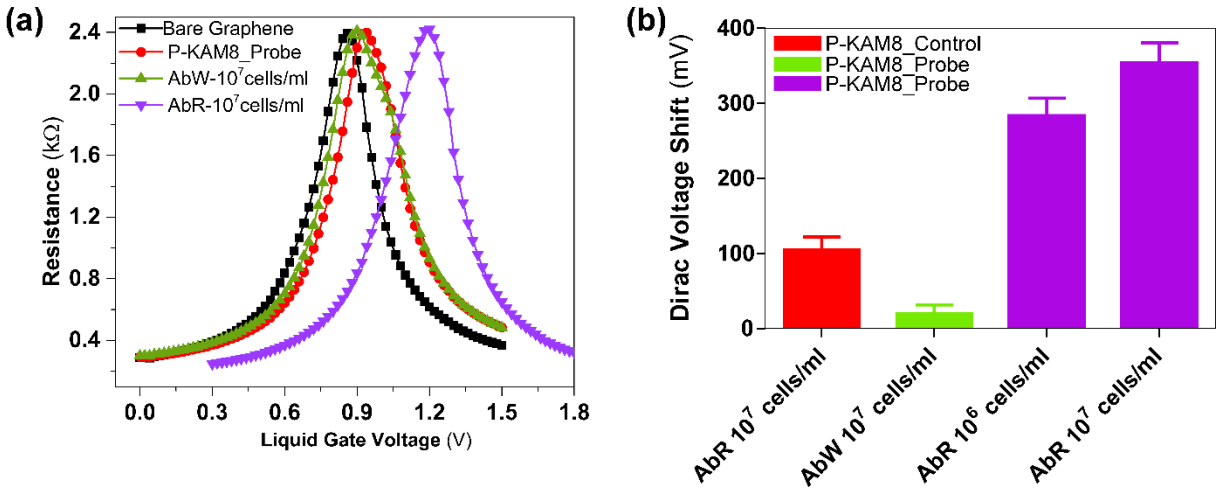

Figure 4. Specific detection results of A. baumannii. *(a) Resistance vs voltage plots of G-FET for detection of A. baumannii with probe peptides KAM8. No shift was observed when the colistin sensitive wt A. baumannii strain (AbW) was exposed to the device, while a ~300 mV shift occurs in the presence of the colistin resistant strain AbR. (b) While P-KAM8_Control does not interact with AbR, and P-KAM-Probe does not interact with AbW, as expected only shifts in Dirac voltage are registered when P-KAM-Probe is combined with AbR. This confirms that devices functionalized with P-KAM8_Probe are specific for AbR with average voltage shifts of 280 mV and 350 mV at concentrations 10^6 and 10^7 cells/ml respectively. (Data represents average and standard deviation of at least 4 independent replicates)*

Lastly, to determine the limit of detection of P-KAM8_Probe functionalized devices, 14 different devices were tested using suspensions of 10^7 cells/ml and 10^6 cells/ml of AbR, obtaining average Dirac voltage shifts of about 350 and 280 mV, respectively (Figure 4b). To reduce the required density, we again employed the electric-field assisted binding method. However, it seems that AbR requires higher voltage pulses as no shift was observed when using -0.5V, the setting that worked for *S. aureus*. Attachment of AbR was detected after applying -1V for 100s, however

this seemed to damage the electrodes in the devices. We found this issue was solved by slowly sweeping the voltage from 0 to -1V with a step voltage of 10mV, resulting in detection of AbR at cell densities as low as 10^4 cells/ml (Figure S7). Taken together, these results demonstrate the potential of the peptide-functionalized G-FETs for specific detection of antibiotic resistant strains of bacterial pathogens. Moreover, our results with at least two bacterial strains (*S. aureus* and colistin resistant *A. baumannii* suggest our new electric-field assisted binding method drastically improves the detection limit and required measurement time.

CONCLUSION

In summary, peptide probes selective to two different pathogenic bacteria were conjugated with pyrene linker and successfully integrated on G-FETs in a single step attachment via non-covalent π-π interaction. The small size, neutral nature (chargeless at ~pH 7), long stability, and easy synthesis make these peptide probes optimal for utilization in G-FET based biosensors. The small size of the bio-recognition element (probes) reduces the effect of Debye screening while their neutral charge reduces the background signal resulting in an enhanced sensitivity to target biomolecules. Furthermore, the pyrene linker commonly used in graphene-based sensing devices can easily be conjugated to these peptides during synthesis. Thereby, pyrene-conjugated peptides can be directly attached to G-FETs in a single step process, eliminating the need for an intermediate linker attachment step and obviates the use of different required solvents. Here we provided a proof of concept utilizing the G-FET functionalized with pyrene-conjugated peptides, to successfully detect species and antibiotic resistant pathogenic bacteria in a single platform. Moreover, the devices showed the detection capability of single cell resolution with a sensitivity of ~56mV/bacterium. Furthermore, by implementing electric field assisted binding of bacteria, the detection speed decreased to 5 minutes from 45 minutes, and the detection limit reduced by 3

orders of magnitude down to 10^4 cells/ml, which is the threshold at which urinary tract infections [43, 44] or bronchoalveolar lavage fluid are indicated to be disease causing.[45, 46]

Further reduction in detection limit below 10^3 cells/ml to meet point of care and clinical requirements [47] is desired and could be obtained by optimizing the device design, PDMS well size as well as the electric field application process. Though, increasing the device size could increase the attachment of bacteria at lower concentrations, it may also reduce the sensitivity of the devices due to non-uniformity (e.g. wrinkles or multiple grains) and impurities with large area graphene.[48, 49] Similarly, large area devices would limit the possibility of miniaturization and multiplexing. Importantly, by applying more cycles of incubation and voltage on the same device we achieved bacterial detection even at 10^3 cells/ml. While, these results showed more variability between replicates, it highlights that further sensitivity improvements are possible. One possible reason for the variability at 10^3 cells/ml is that in the 20µL sample that is added to the device there are only ~20 bacterial cells present. As described above the sensing area is small (10 x 40 µm) compared to the PDMS well that holds the 20µL sample (2.5 x 2.5 mm). This means that the bacterial density is just 3.2/mm^2 and thus even with the applied electric field the travel distance of a bacterium to the probes at the graphene surface remains far, with potential for other locations of attachment. Hence, optimizing the geometry of the PDMS well, resist surface and voltage application process, and/or integrating the system into a PDMS microfluidics chip could help to further reduce the detection limit. Nonetheless, our results show that the combination of pyrene modified peptides along with highly sensitive G-FETs are capable to solve major challenges faced in label free biosensors of bacteria, which potentially opens up a pathway to the development of a reliable platform for point of care diagnostics of infectious diseases.

METHODS

G-FET Fabrication and Characterization

G-FETs were fabricated on CVD monolayer graphene transferred over SiO_2/Si substrates. Monolayer graphene was grown on copper via low pressure chemical vapor deposition. The copper foil (Alfa Aesar) was pre-treated in Ni etchant (Transene) to remove any coatings or oxide layers from its surface. The tube furnace was evacuated to a read pressure of 200 mTorr with a constant flow of H_2 (10 sccm). Prior to growth, the foil was annealed at 1010 ^oC (ramp rate 25 ^oC/min) for 35 minutes. Growth was done at 1010 ^oC with 68 sccm of H_2 and 3.5 sccm of CH_4 for 15 minutes. After growth, a polymethyl methacrylate (PMMA) layer was spin coated on one side of the copper foil and baked for 60 seconds at 60 ^oC. To facilitate smooth and fast etching of the copper foil, the backside graphene was etched out using oxygen plasma with 60 watt power for 60 seconds. The exposed copper was etched away in Ni etchant for 2h at 60 ^oC. The remaining PMMA/graphene structure was washed in 2 water baths, the first water bath for 60 seconds and the second for 30 minutes, to rinse away left over etchant. The PMMA/graphene was transferred onto SiO_2/Si chips of size 1 x 1 cm. Any leftover water was slowly dried out with nitrogen gas, and finally the PMMA was dissolved in acetone vapors; isopropanol alcohol (Fischer) was used for a final wash. The chips were baked at 300 ^oC for 8h in vacuum followed by deposition of 3 nm AlOx at room temperature by evaporating aluminum at oxygen pressure of 7.5×10^5 mbar. Substrates were baked at 175 ^oC for 10 minutes before lithography process. The electrodes patterning was done using bilayer photoresist (LOR1A/S1805) and laser mask writer (Heidelberg Instruments) followed by Au/Cr (45 nm/5 nm) deposition and lift off using remover PG (MicroChem). After that the graphene patterning was done with lithography using same bilayer resist and oxygen plasma etching. Devices were cleaned with remover PG and rinsed with IPA, DI water and dried with

Argon. In order to protect the electrodes and edges of the graphene for liquid gating, photolithography was done using S1805 to open the sensing area (10 x 40 µm) and contact pads while leaving remaining chip covered. The developing time was increased to 90 seconds to etch away the AlOx layer deposited in the beginning to protect the graphene from photoresist. Finally, the chips were baked at 150 ^{o}C for 5 minutes and then temperature increased to 200 ^{o}C and baked for 5 more minutes to harden the photoresist. To perform the measurement of the devices, two PDMS wells of size 2.5 x 2.5 mm were fabricated and placed over the chip having two sets of the devices with three devices in each well. 20 µL of diluted 0.01x PBS was filled and a platinum wire of 0.5 mm diameter was used for liquid gating.

SI Peptide synthesis

Solid phase peptide synthesis was performed on a rink amide resin using Fmoc chemistry. An alloc-protected diaminopropionic acid residue was installed at the C-terminus for on-resin coupling of pyrene. The alloc protecting group was selectively removed by tetrakis (triphenylphosphine) palladium (0) and phenylsilane in DCM for 1 hour. 2 equivalents of 1-Pyrenebutyric acid N-hydroxysuccinimide ester in 20% v/v DIPEA/DMF was added. The coupling was done in 2 hours at room temperature. The peptides were cleaved off resin and globally deprotected with 90% TFA, 5% H_2O, 2.5% triisopropylsilane, 2.5% 1,2-ethanedithiol for 2 hours. Crude peptides were obtained via cold ether precipitation and purified by RP-HPLC. For cysteine alkylation, the peptides were treated with 3 equivalents of APBA-IA or IA in 5% v/v DIPEA/DMF for 3 hours and purified via RP-HPLC. All peptides were characterized with LC-MS to confirm their identities and excellent purities (>95%).

Bacterial strains and culture conditions

Detections were made using the following strains: *S. aureus* (ATCC 6538), wild-type *A. baumannii* (AB5075),[50] colistin resistant and LOS deficient *A. baumannii* (5075 LOS−),[51] *B. subtilis*, and *E. coli (BL 21)*. All bacteria were cultured overnight in LB broth at 37 °C with 220 rpm constant shaking. The overnight culture was diluted 10^2 times in fresh media and grown to an OD_{600} of 0.5-1.0. These fresh cultures were then washed and diluted with 1x PBS (pH 7.4) buffer to obtain the desired concentrations.

ASSOCIATED CONTENTS

Supplementary Information

G-FET characteristics obtained for detection of *S. aureus* with bare graphene. Stability test results tested by storing functionalized G-FETs for 24 hours in PBS and detection of *S. aureus* performed. Observed Dirac voltage shift with number of bacteria attached achieved by electric field assisted binding at lower concentration 10^4 and 10^5 cells/ml of *S. aureus*. Negative Control experiments for electric field assisted binding. Negative control test with P-KAM8_Control and *A. baumannii*. Observed Dirac voltage shift with number of bacteria in detection of *A. baumannii*. Dirac voltage shift with electric field assisted binding of *A. baumannii* to detect lower concentration i.e. 10^4 and 10^5 cells/ml.

AUTHOR INFORMATION

Corresponding Authors

*Email: ks.burch@bc.edu

*Email:vanopijn@bc.edu

*Email:gaojc@bc.edu

Author contributions

K.S.B, J.G. and T.v.O conceived the project and designed the experiments. N.K. performed fabrication, functionalization, and testing of G-FETs, M.G. and N.B. assisted in the fabrication of devices. W.W. synthesized the peptides, W.W. and J.O-M. performed bacterial cultures, M.C. assisted in measurements, K.H. performed the growth of graphene on copper and helped in transferring over to SiO_2/Si substrates, X.L. supervised the graphene growth and transfer process, N.K, J.O-M., W.W. K.S.B, J.G., and T.v.O analyzed the data and wrote the manuscript.

† These authors contributed equally.

ACKNOWLEDGMENTS

N.K, T.vO and J.O-M were supported by R01-AI110724 and U01-AI124302. W.W. and J.G. acknowledge the National Institutes of Health financial support through grants R01-GM102735 and R01-GM124231. M.G. and K.S.B. acknowledge support from the National Science Foundation, through grant DMR-1709987. N.B. acknowledges support from the National Science Foundation, through grant BIO-1460628.

REFERENCES

1. Filice, G. A.; Nyman, J. A.; Lexau, C.; Lees, C. H.; Bockstedt, L. A.; Como-Sabetti, K.; Lesher, L. J.; Lynfield, R., Excess costs and utilization associated with methicillin resistance for patients with Staphylococcus aureus infection. *Infection Control & Hospital Epidemiology* **2010,** *31* (4), 365-373.
2. Control, C. f. D.; Prevention, *Antibiotic resistance threats in the United States, 2013*. Centres for Disease Control and Prevention, US Department of Health and …: 2013.
3. López-Góngora, S.; Puig, I.; Calvet, X.; Villoria, A.; Baylina, M.; Munoz, N.; Sanchez-Delgado, J.; Suarez, D.; Garcia-Hernando, V.; Gisbert, J. P., Systematic review and meta-analysis: susceptibility-guided versus empirical antibiotic treatment for Helicobacter pylori infection. *Journal of Antimicrobial Chemotherapy* **2015,** *70* (9), 2447-2455.
4. Scholte, J.; Duong, H.; Linssen, C.; Van Dessel, H.; Bergmans, D.; van der Horst, R.; Savelkoul, P.; Roekaerts, P.; van Mook, W., Empirical antibiotic therapy for pneumonia in intensive care units: a multicentre, retrospective analysis of potentially pathogenic microorganisms identified by endotracheal aspirates cultures. *European Journal of Clinical Microbiology & Infectious Diseases* **2015,** *34* (11), 2295-2305.
5. Varadi, L.; Luo, J. L.; Hibbs, D. E.; Perry, J. D.; Anderson, R. J.; Orenga, S.; Groundwater, P. W., Methods for the detection and identification of pathogenic bacteria: past, present, and future. *Chemical Society Reviews* **2017,** *46* (16), 4818-4832.

6. Syal, K.; Mo, M.; Yu, H.; Iriya, R.; Jing, W.; Guodong, S.; Wang, S.; Grys, T. E.; Haydel, S. E.; Tao, N., Current and emerging techniques for antibiotic susceptibility tests. *Theranostics* **2017,** *7* (7), 1795.
7. Jenkins, S. G.; Schuetz, A. N. In *Current concepts in laboratory testing to guide antimicrobial therapy*, Mayo Clinic Proceedings, Elsevier: 2012; pp 290-308.
8. van Belkum, A.; Bachmann, T. T.; Lüdke, G.; Lisby, J. G.; Kahlmeter, G.; Mohess, A.; Becker, K.; Hays, J. P.; Woodford, N.; Mitsakakis, K.; Moran-Gilad, J.; Vila, J.; Peter, H.; Rex, J. H.; Dunne, W. M.; the, J. A. M. R. R. D. T. W. G. o. A. R.; Rapid Diagnostic, T., Developmental roadmap for antimicrobial susceptibility testing systems. *Nature Reviews Microbiology* **2019,** *17* (1), 51-62.
9. Zumla, A.; Al-Tawfiq, J. A.; Enne, V. I.; Kidd, M.; Drosten, C.; Breuer, J.; Muller, M. A.; Hui, D.; Maeurer, M.; Bates, M., Rapid point of care diagnostic tests for viral and bacterial respiratory tract infections—needs, advances, and future prospects. *The Lancet Infectious Diseases* **2014,** *14* (11), 1123-1135.
10. Huang, T.-H.; Ning, X.; Wang, X.; Murthy, N.; Tzeng, Y.-L.; Dickson, R. M., Rapid cytometric antibiotic susceptibility testing utilizing adaptive multidimensional statistical metrics. *Analytical chemistry* **2015,** *87* (3), 1941-1949.
11. Boucher, H. W.; Bakken, J. S.; Murray, B. E., The United Nations and the urgent need for coordinated global action in the fight against antimicrobial resistance. *Annals of internal medicine* **2016,** *165* (11), 812-813.
12. Fu, W.; Jiang, L.; van Geest, E. P.; Lima, L. M.; Schneider, G. F., Sensing at the surface of graphene field-effect transistors. *Advanced Materials* **2017,** *29* (6), 1603610.
13. Ping, J.; Vishnubhotla, R.; Vrudhula, A.; Johnson, A. C., Scalable production of high-sensitivity, label-free DNA biosensors based on back-gated graphene field effect transistors. *ACS nano* **2016,** *10* (9), 8700-8704.
14. Xu, S.; Zhan, J.; Man, B.; Jiang, S.; Yue, W.; Gao, S.; Guo, C.; Liu, H.; Li, Z.; Wang, J., Real-time reliable determination of binding kinetics of DNA hybridization using a multi-channel graphene biosensor. *Nature communications* **2017,** *8*, 14902.
15. Fu, W.; Feng, L.; Panaitov, G.; Kireev, D.; Mayer, D.; Offenhäusser, A.; Krause, H.-J., Biosensing near the neutrality point of graphene. *Science advances* **2017,** *3* (10), e1701247.
16. Huang, Y.; Dong, X.; Liu, Y.; Li, L.-J.; Chen, P., Graphene-based biosensors for detection of bacteria and their metabolic activities. *Journal of Materials Chemistry* **2011,** *21* (33), 12358-12362.
17. Thakur, B.; Zhou, G.; Chang, J.; Pu, H.; Jin, B.; Sui, X.; Yuan, X.; Yang, C.-H.; Magruder, M.; Chen, J., Rapid detection of single E. coli bacteria using a graphene-based field-effect transistor device. *Biosensors and Bioelectronics* **2018,** *110*, 16-22.
18. Wu, G.; Dai, Z.; Tang, X.; Lin, Z.; Lo, P. K.; Meyyappan, M.; Lai, K. W. C., Graphene Field-Effect Transistors for the Sensitive and Selective Detection of Escherichia coli Using Pyrene-Tagged DNA Aptamer. *Advanced healthcare materials* **2017,** *6* (19), 1700736.
19. Templier, V.; Roux, A.; Roupioz, Y.; Livache, T., Ligands for label-free detection of whole bacteria on biosensors: A review. *TrAC Trends in Analytical Chemistry* **2016,** *79*, 71-79.
20. Rubab, M.; Shahbaz, H. M.; Olaimat, A. N.; Oh, D.-H., Biosensors for rapid and sensitive detection of Staphylococcus aureus in food. *Biosensors and Bioelectronics* **2018,** *105*, 49-57.
21. Donnelly, M.; Mao, D.; Park, J.; Xu, G., Graphene field-effect transistors: the road to bioelectronics. *Journal of Physics D: Applied Physics* **2018,** *51* (49), 493001.

22. Mannoor, M. S.; Tao, H.; Clayton, J. D.; Sengupta, A.; Kaplan, D. L.; Naik, R. R.; Verma, N.; Omenetto, F. G.; McAlpine, M. C., Graphene-based wireless bacteria detection on tooth enamel. *Nature communications* **2012,** *3*, 763.
23. Soares, J.; Morin, K.; Mello, C. *Antimicrobial peptides for use in biosensing applications*; ARMY NATICK RESEARCH DEVELOPMENT AND ENGINEERING CENTER MA: 2004.
24. Mannoor, M. S.; Zhang, S.; Link, A. J.; McAlpine, M. C., Electrical detection of pathogenic bacteria via immobilized antimicrobial peptides. *Proceedings of the National Academy of Sciences* **2010,** *107* (45), 19207-19212.
25. Etayash, H.; Jiang, K.; Thundat, T.; Kaur, K., Impedimetric detection of pathogenic gram-positive bacteria using an antimicrobial peptide from class IIa bacteriocins. *Analytical chemistry* **2014,** *86* (3), 1693-1700.
26. Liu, X.; Marrakchi, M.; Xu, D.; Dong, H.; Andreescu, S., Biosensors based on modularly designed synthetic peptides for recognition, detection and live/dead differentiation of pathogenic bacteria. *Biosensors and Bioelectronics* **2016,** *80*, 9-16.
27. McGregor, D. P., Discovering and improving novel peptide therapeutics. *Current opinion in pharmacology* **2008,** *8* (5), 616-619.
28. Zasloff, M., Antimicrobial peptides of multicellular organisms. *nature* **2002,** *415* (6870), 389.
29. Chen, T.-Y.; Loan, P. T. K.; Hsu, C.-L.; Lee, Y.-H.; Wang, J. T.-W.; Wei, K.-H.; Lin, C.-T.; Li, L.-J., Label-free detection of DNA hybridization using transistors based on CVD grown graphene. *Biosensors and Bioelectronics* **2013,** *41*, 103-109.
30. Kireev, D.; Brambach, M.; Seyock, S.; Maybeck, V.; Fu, W.; Wolfrum, B.; Offenhäusser, A., Graphene transistors for interfacing with cells: towards a deeper understanding of liquid gating and sensitivity. *Scientific reports* **2017,** *7* (1), 6658.
31. Mulyana, Y.; Uenuma, M.; Okamoto, N.; Ishikawa, Y.; Yamashita, I.; Uraoka, Y., Alterations in ambipolar characteristic of graphene due to adsorption of Escherichia coli bacteria. *Journal of Physics D: Applied Physics* **2018,** *51* (11), 115102.
32. Georgakilas, V.; Otyepka, M.; Bourlinos, A. B.; Chandra, V.; Kim, N.; Kemp, K. C.; Hobza, P.; Zboril, R.; Kim, K. S., Functionalization of graphene: covalent and non-covalent approaches, derivatives and applications. *Chemical reviews* **2012,** *112* (11), 6156-6214.
33. Wang, C.; Kim, J.; Zhu, Y.; Yang, J.; Lee, G.-H.; Lee, S.; Yu, J.; Pei, R.; Liu, G.; Nuckolls, C., An aptameric graphene nanosensor for label-free detection of small-molecule biomarkers. *Biosensors and Bioelectronics* **2015,** *71*, 222-229.
34. McCarthy, K. A.; Kelly, M. A.; Li, K.; Cambray, S.; Hosseini, A. S.; van Opijnen, T.; Gao, J., Phage display of dynamic covalent binding motifs enables facile development of targeted antibiotics. *Journal of the American Chemical Society* **2018,** *140* (19), 6137-6145.
35. Kuang, Z.; Kim, S. N.; Crookes-Goodson, W. J.; Farmer, B. L.; Naik, R. R., Biomimetic Chemosensor: Designing Peptide Recognition Elements for Surface Functionalization of Carbon Nanotube Field Effect Transistors. *ACS Nano* **2010,** *4* (1), 452-458.
36. Liu, C.; Hu, Y.-L.; Deng, W.-J.; Pan, Q.-S.; Yi, J.-T.; Chen, T.-T.; Chu, X., A graphene oxide nanosensor enables the co-delivery of aptamer and peptide probes for fluorescence imaging of a cascade reaction in apoptotic signaling. *Analyst* **2018,** *143* (1), 208-214.
37. Wu, J.-B.; Lin, M.-L.; Cong, X.; Liu, H.-N.; Tan, P.-H., Raman spectroscopy of graphene-based materials and its applications in related devices. *Chemical Society Reviews* **2018,** *47* (5), 1822-1873.

38. Monteiro, J. M.; Fernandes, P. B.; Vaz, F.; Pereira, A. R.; Tavares, A. C.; Ferreira, M. T.; Pereira, P. M.; Veiga, H.; Kuru, E.; VanNieuwenhze, M. S., Cell shape dynamics during the staphylococcal cell cycle. *Nature communications* **2015,** *6*, 8055.
39. Nikkhoo, N.; Cumby, N.; Gulak, P. G.; Maxwell, K. L., Rapid Bacterial Detection via an All-Electronic CMOS Biosensor. *PloS one* **2016,** *11* (9), e0162438.
40. Formisano, N.; Bhalla, N.; Heeran, M.; Martinez, J. R.; Sarkar, A.; Laabei, M.; Jolly, P.; Bowen, C. R.; Taylor, J. T.; Flitsch, S., Inexpensive and fast pathogenic bacteria screening using field-effect transistors. *Biosensors and Bioelectronics* **2016,** *85*, 103-109.
41. Belgrader, P.; Benett, W.; Hadley, D.; Richards, J.; Stratton, P.; Mariella, R.; Milanovich, F., PCR detection of bacteria in seven minutes. *Science* **1999,** *284* (5413), 449-450.
42. Kłodzińska, E.; Szumski, M.; Dziubakiewicz, E.; Hrynkiewicz, K.; Skwarek, E.; Janusz, W.; Buszewski, B., Effect of zeta potential value on bacterial behavior during electrophoretic separation. *Electrophoresis* **2010,** *31* (9), 1590-1596.
43. Nicolle, L. E.; Bradley, S.; Colgan, R.; Rice, J. C.; Schaeffer, A.; Hooton, T. M., Infectious Diseases Society of America guidelines for the diagnosis and treatment of asymptomatic bacteriuria in adults. *Clinical infectious diseases* **2005**, 643-654.
44. Doern, C. D.; Richardson, S. E., Diagnosis of urinary tract infections in children. *Journal of clinical microbiology* **2016,** *54* (9), 2233-2242.
45. Kalil, A. C.; Metersky, M. L.; Klompas, M.; Muscedere, J.; Sweeney, D. A.; Palmer, L. B.; Napolitano, L. M.; O'Grady, N. P.; Bartlett, J. G.; Carratalà, J., Management of adults with hospital-acquired and ventilator-associated pneumonia: 2016 clinical practice guidelines by the Infectious Diseases Society of America and the American Thoracic Society. *Clinical Infectious Diseases* **2016,** *63* (5), e61-e111.
46. Miller, J. M.; Binnicker, M. J.; Campbell, S.; Carroll, K. C.; Chapin, K. C.; Gilligan, P. H.; Gonzalez, M. D.; Jerris, R. C.; Kehl, S. C.; Patel, R., A guide to utilization of the microbiology laboratory for diagnosis of infectious diseases: 2018 update by the Infectious Diseases Society of America and the American Society for Microbiology. *Clinical Infectious Diseases* **2018,** *67* (6), e1-e94.
47. Habimana, J. d. D.; Ji, J.; Sun, X., Minireview: trends in optical-based biosensors for point-of-care bacterial pathogen detection for food safety and clinical diagnostics. *Analytical Letters* **2018,** *51* (18), 2933-2966.
48. Caillier, C.; Ki, D.-K.; Lisunova, Y.; Gaponenko, I.; Paruch, P.; Morpurgo, A. F., Identification of a strong contamination source for graphene in vacuum systems. *Nanotechnology* **2013,** *24* (40), 405201.
49. Mates, S. M.; Eisenberg, E. S.; Mandel, L. J.; Patel, L.; Kaback, H. R.; Miller, M. H., Membrane potential and gentamicin uptake in Staphylococcus aureus. *Proceedings of the National Academy of Sciences* **1982,** *79* (21), 6693-6697.
50. Jacobs, A. C.; Thompson, M. G.; Black, C. C.; Kessler, J. L.; Clark, L. P.; McQueary, C. N.; Gancz, H. Y.; Corey, B. W.; Moon, J. K.; Si, Y., AB5075, a highly virulent isolate of Acinetobacter baumannii, as a model strain for the evaluation of pathogenesis and antimicrobial treatments. *MBio* **2014,** *5* (3), e01076-14.
51. Boll, J. M.; Crofts, A. A.; Peters, K.; Cattoir, V.; Vollmer, W.; Davies, B. W.; Trent, M. S., A penicillin-binding protein inhibits selection of colistin-resistant, lipooligosaccharide-deficient Acinetobacter baumannii. *Proceedings of the National Academy of Sciences* **2016,** *113* (41), E6228-E6237.